Mem. Fac. Fish. Kagoshima Univ.,
Vol. 55, pp. 13~26（2006）

Chlorophyll *a* Distribution Deduced from MODIS Ocean Color Data and its Characteristics around Hyuganada

Gathot Winarso, Kazunori Hosotani, and Hiroyuki Kikukawa*

Key words : chlorophyll *a*, SST, MODIS, PIV, Hyuganada

Abstract

The Aqua satellite loaded with MODIS system surveys visible and infrared radiation in 36 wave bands, providing simultaneous images of chlorophyll *a* concentration and sea surface temperature (SST) in the upper layer of the sea. For the first time, synoptic chlorophyll *a* concentration data and SST images become to be available. The purpose of this paper is to explore the advantage of ocean color data from MODIS including chlorophyll *a* concentration and SST to interpret the oceanographic processes. This research was performed in Hyuganada located in the east coast of Kyushu Island. The synoptic image of chlorophyll *a* concentration and SST was found to be a great tool to understand the interaction between water temperature and biological process. From the chlorophyll *a* image deduced from MODIS data, we could recognize the front of water mass in summer more clearly than from the SST images. The eddy could be interpreted well by the chlorophyll *a* images. By the particle image velocimetry (PIV) analysis, the chlorophyll *a* images could be used to make out ocean flow field including direction and velocity of the current. The seasonal changes of the chlorophyll *a* concentration are also discussed.

1. Introduction

As we know, 70 % of the earth's surface is covered by water, in the northern hemisphere 60% and in the southern hemisphere 80%[1]. Oceans play an important role in the earth system by the interaction with atmosphere. Oceans are dynamical environments, but they do not consist of their own environments alone, and rather interact with atmosphere, land ice and living organisms. They are part of the interconnected systems of the earth. Furthermore, humans influence the oceans and are also influenced by them. The natural fluid motions occurring in these systems are parts of geophysical fluid dynamics whose full-scale experimentation must be ruled out, and investigations are conducted via laboratory experiments and numerical models. Observation of the geophysical flow also faces the difficulty in the length and times scale that is impractically large.[2]

Advances in satellite imagery and other methods of satellite remote sensing provide the method of synoptic field investigation. Also, remote sensing provides a valuable perspective concerning broad-scale, dynamic patterns that are difficult to examine in detail using only point measurements. Although they are usually restricted to a specific level in the vertical or vertically integrated quantities, remotely sensed data can be especially valuable for studying the phenomena over large scale areas, and satellite sensors are advantageous to regular and simultaneous observation.[3] One of the

鹿児島大学水産学部環境情報科学講座 (Department of Environmental and Information Sciences, Faculty of Fisheries, Kagoshima University, 4-50-20 Shimoarata, Kagoshima 890-0056, Japan)
* Corresponding author, Email: kikukawa@fish.kagoshima-u.ac.jp

advances of the remote sensing technology concerns MODIS data. MODIS is the abbreviation of *Moderate Resolution Imaging Spectroradiometer*, moderate in spatial resolution and spectral resolution. With 36 bands, MODIS will improve our understanding of global dynamics and processes occurring on the land, in the ocean, and in the lower atmosphere. MODIS helps to understand interrelationships among them using measurements from satellite-based instruments.[4)]

The truly synoptic chlorophyll *a* concentration and SST images are available for the first time in MODIS data. Total primary production, defined as the amount of organic matters produced in a given period of time[5)] through the photosynthetic process, is proportional to the chlorophyll *a* concentration in the surface layer of the ocean. Primary production increased by the nutrients supplied from coastal river and upwelling processes is linked to fishery yield. Variables such as phytoplankton and primary production are often better predictors for fishery yield than physical, chemical and hydrological variables.[6)] The purpose of this paper is to explore the advantage of MODIS Ocean Color data by the derivation of useful information data such as chlorophyll *a* concentration and SST from raw data and then interpret the oceanographic processes such as current front, eddy current and upwelling, also the current direction and velocity by using PIV analysis. We hope that the results could be one of the useful application of the oceanic images deduced from remote sensing data and would help to promote a better understanding of the ocean.

2. Study Area and Methods

2.1. Study Area

The research was done in the sea near the east coast of Kyushu Island where the Kuroshio Current flows (Fig. 1). The Kuroshio flows out to the Pacific Ocean from the East China Sea through Tokara Strait, proceeds northeastward along the east coats of Kyushu Island and flows along south coast of Japan, and commonly around 36° N it turns eastward[7)] as shown in Fig. 1. The Kuroshio volume transport changes seasonally and inter-annually, maximum in summer and minimum in autumn, while its annual pattern changes year by years. These seasonal changes vary the Kuroshio axis in shape and position, generating a meandering and eddy in this area. Because of this process, there is the water mass mixing in this area, which affects to the chlorophyll *a* concentration and SST.

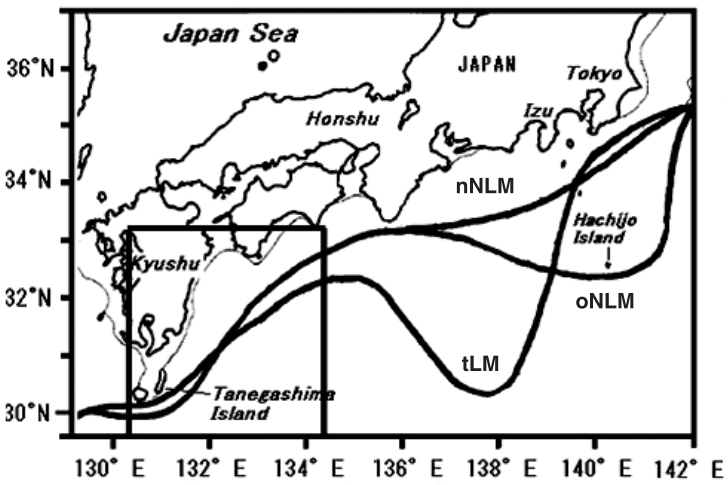

Fig. 1. Location of the study area (surrounded by square box) and typical path of the Kuroshio classified to typical large meander (tLM) and nearshore/offshore non-large meander (n/o NLM)[7)] .

2.2. Data

Most of the data used in this study are derived from MODIS. MODIS is a key instrument aboard the Terra (EOS AM) and Aqua (EOS PM) Satellites. Terra MODIS and Aqua MODIS are viewing the entire Earth's surface every 1 or 2 days, acquiring data in 36 spectral bands, or groups of wavelengths.

The data was downloaded from the Goddard Earth Science, the Data and Information Service Center, the National Aeronautics and Space Administration (NASA), the United States of America. The downloaded

data is level 1A. For ocean color application, we used from band 8 to band 16, and for SST, band 31 and band 32 were used.

2.3. Radiometric Correction

At the ocean, about 10% of the total light detected by a satellite is water-leaving radiance, while the other 90% of the light is due to atmospheric effects. Corrections to the data must be necessary to remove this atmospheric radiance.

After the radiance signal has been corrected for atmospheric light scattering, the signal is then corrected for the solar zenith angle. This gives us the normalized water-leaving radiance, which is the radiance that would be measured when the surface of the ocean is flat, the sun at zenith is directly overhead and the atmosphere is absent. The normalized water-leaving radiances are then used in algorithms to produce geophysical values, such as chlorophyll *a* concentration.

First, we convert radiance L into reflectance ρ, because it is more convenient to work with dimension-less reflectance rather than radiance, and because the new sensors may be calibrated in reflectance instead of radiance.

$$\rho = \pi L / F0 \cos(\theta_0),$$

where F0 is the extraterrestrial solar irradiance and θ_0 denotes the solar zenith angle.

We can write the total reflectance, measured at the top of the atmosphere in the each band as

$$\rho_t = \rho_r + (\rho_a + \rho_{ra}) + t\rho_{wc} + t\rho_g + t\rho_w,$$

where ρ_r is the reflectance resulting from multiple scattering by air molecules (Rayleigh scattering) in the absence of aerosols, ρ_a the reflectance resulting from multiple scattering by aerosols in the absence of air, ρ_{ra} the interaction between molecular and aerosol scattering, ρ_g the direct solar beam reflectance, ρ_{wc} reflectance from the (rough) ocean surface, ρ_w the water-leaving reflectance and t denotes the diffuse transmittance of the atmosphere. The term ρ_{ra} accounts for the interaction between Rayleigh and aerosol scattering, e.g., photons first scattered by the air then scattered by aerosols, or photons first scattered by aerosols then by the air. This term is set to zero in the single-scattering case, in which photons are assumed be scattered only once.[8)]

The process of radiometric correction can be seen in Fig. 2. From this process we got ρ_w and removed other reflectances, but this value is still affected by solar zenith angle and atmosphere from just above seawater to sensor. To remove this effect, we normalize ρ_w by the equation:

$$n\rho_w = \rho_w / t(\theta_0, \lambda),$$

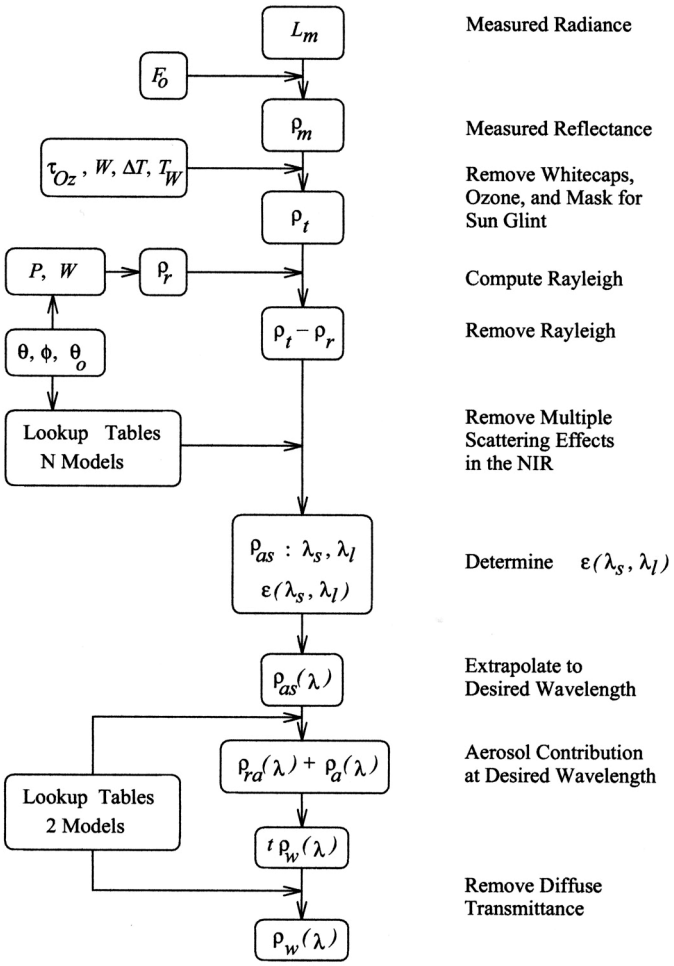

Fig. 2. Flow diagram to derive the normalized water-leaving radiance algorithm processes.[9)]

$t(\theta_0, \lambda) = \exp[- \{(\tau r(\lambda)/2) + tOz(\lambda)\} (1/\cos(\theta_0))]$,

where τr and τOz are Rayleigh and ozone optical thickness. Then we converted back to radiance by the following equation:

$nL_w = n\rho_w F0 / \pi$.

Finally, we got the normalized water leaving radiance[9] nL_w. The normalized water-leaving radiances are the radiance that would be measured when the surface of the ocean is flat and the sun is at zenith (directly overhead) and the atmosphere is absent. The normalized water-leaving radiances are then used in algorithms to produce geophysical values, such as chlorophyll concentration. We have processed the radiometric correction using SeaDas Software.

2.4. Chlorophyll *a* Concentration

Chlorophyll *a* concentration algorithm was developed based on semi-analytical, bio-optical of remote sensing reflectance (Rrs). The Rrs is calculated by the equation bellow:

$Rrs(\lambda) = nLw(\lambda) / F0(\lambda)$,

where F0(λ) is mean solar irradiance. The "best" value of F0(λ) should be computed as a full band wavelength of nLw(λ), but nominal value of F0(λ) is computed from a 10-nm square distribution, centered at the sensor nominal wavelength. For standard processing, the nLw(λ) is reported as a nominal band value. From Rrs(λ) we calculated the chlorophyll *a* concentration Ca by the standard algorithm explained in MODIS Ocean Color Discipline website:

$Ca = 10^{CR}$,

$CR = 0.283 - 2.753R + 1.457R^2 + 0.659R^3 - 1.403R^4$,

where $R = \log_{10}((Rrs443 > Rrs488)/ Rrs551)$ and (Rrs443> Rrs488) is a shorthand representation meaning that the argument of the logarithm is the maximum of two values.

2.5. Sea Surface Temperature

The basis for the MODIS V.2 pre-launch SST algorithm is the Miami Pathfinder SST (mpfsst) algorithm, developed at University of Miami's Rosenstiel School of Marine and Atmospheric Science (UM-RSMAS)[10]:

$SST = c1 + c2 * T31 + c3 * T3132 + c4 * (\sec(\theta) - 1) * T3132$,

where T31 is the band 31 brightness temperature (BT), T3132 is (Band32 - Band31) BT difference and θ is the satellite zenith angle.

This algorithm corrects the effect of atmospheric vapor using the difference between the brightness temperatures (T3132) for the 11 and 12 μm bands (MODIS Bands 31 and 32). Coefficients are differently determined if T3132 is greater or less than 0.7K. In application, the coefficients are then weighted by measured T3132[10]. Coefficients for the MODIS Band 31 and 32 SST retrieval algorithms are derived using ECMWF (European Centre for Medium-Range Weather Forecasts) assimilation model of marine atmospheres accounting atmospheric properties and variability. The coefficients are shown in Table 1.

Table 1. The coefficients c1 to c4 for the MODIS band 31 and 32 SST retrieval algorithms derived from ECMWF assimilation model of marine atmospheres.

	T30 - T31 ≤ 0.7	T30 - T31 > 0.7
c1	1.11071	1.196099
c2	0.9586865	0.9888366
c3	0.1741229	0.1300626
c4	1.876752	1.62712

2.6. Particle Image Velocimetry

PIV is an image-based technique developed over the last decade to determine two-dimensional distributions of flow velocity in laboratory experiments. It entails particle-seeding in an illuminated flow region, recording a sequence of images of the particles moving in the flow region, then processing the images by means of statistical-correlation analysis to produce a field of

velocity vectors. PIV identifies patterns in small areas (called interrogation areas) and determines the displacements of those patterns between successive images. Thus, it is potentially useful for determining the velocity vectors of whole fields of moving water mass. The essential aspect of PIV is the accurate measurement of pattern displacements during a known period between consecutive images. Velocities are determined by dividing the displacements by the period between the images. An entire vector field is obtained by repeating this procedure for a grid of interrogation areas encompassing the flow field image.[11)]

PIV relies on an image-processing scheme that performs statistical analysis of the images. The analytical algorithm used for our study is essentially the same as the one developed for satellite imagery of cloud motion.[12)] The analysis involves an interrogation procedure that cross-correlates the distributions of chlorophyll *a* concentration in a pair of images.

Cross-correlation is performed between an interrogation area centered in one point in the first image and the one within a search area of the second image. The size and shape of the search area is chosen on the basis of prior knowledge about the flow field. Cross-correlation is successively conducted for all the interrogation area between two images. The displacement of the original location is determined when the correlation coefficient is maximal.

3. Characteristics of Hyuganada

3.1. Chlorophyll *a* Concentration

The chlorophyll *a* concentration image derived from MODIS data is shown in Plate 1a. This image was derived from MODIS Aqua sensor, acquired at 27th July 2005, calculated using chl_oc3 algorithm, processed by SeaDas software.

From this image we got the spatial distribution of chlorophyll *a* concentration value in each pixel. The chlorophyll *a* concentration was high along the east coast of Kyushu Island from Osumi Peninsula to the south coast of Sikoku Island, and higher inside the Bungo Channel. The concentration was more than 0.5 mg/m^3, was more than 1 mg/m^3 just near the coast, and decreases extremely to less than 0.4 mg/m^3 at about 10 km off from the coast. In the area far from coast, we found the concentration less than 0.2 mg/m^3. The chlorophyll *a* concentration deduced from MODIS data using standard algorithm is almost the same as one obtained by field survey measurement.

Takahashi and Kawamura[13)] reported that chlorophyll *a* concentration measured by JODC was between 0.1 and more than 1 mg/m^3 on the coastal water and between less than 0.1 and 0.7 mg/m^3 on the Kuroshio water in summer season. By using SeaWiFS, Miyashita[14)] examined the chlorophyll *a* concentration along south coast of Japan. That data was 5 years data set (1998-2002), global area coverage (GAC) of SeaWiFS data with 9.28 km resolution. She concluded that the chlorophyll *a* concentration was relatively high (>0.5 mg/m^3) in the coastal region and low (<0.5 mg/m^3) in the offshore region. During 5 years, the high chlorophyll *a* concentration more than 2.5 mg/m^3 was found all along the south of Japan coast except Kyushu and Shikoku Islands and the Kii Peninsula, where it is close to 2.0 mg/m^3. In the offshore region the chlorophyll *a* concentration is between 0.01 and 0.5 mg/m^3.

The valid result of chlorophyll *a* concentration is generated by the development of the algorithm, especially the atmospheric correction, that can be used for almost all regions. However, the result is good only in oceanic water characterized as Case-1, in which the optical properties are dominated by chlorophyll and covary with detrital pigments. In the coastal water

characterized as Case-2, in which other substances such as gelbstoff, suspended sediments, coccolithophores, detritus and bacteria, also affect the optical property, there is special algorithm to derive right chlorophyll *a* concentration.[15)]

Darecki and Stramski[16)] evaluated the performance of standard Moderate Resolution Imaging Spectroradiometer (MODIS) and Sea-viewing Wide Field-of-view Sensor (SeaWiFS) Ocean Color (in-water) algorithms using an extensive bio-optical data set from field measurements in the Baltic Sea, which represents an example of optically complex Case-2 waters with high concentration of colored dissolved organic matter (CDOM). They concluded that their analysis revealed a systematic and large overestimation of chlorophyll for the MODIS and SeaWiFS algorithms. This result includes the semi-analytical algorithm based on the model of Carder *et al*,[15)] which was designed to have an improved performance in Case-2 waters.

We found the high concentration more than 2 mg/m^3 in the coastal area especially inside of Bungo Channel. Miyashita[14)] also found there the high concentration. Those results should be clarified by field survey measurement in the area, which indicates Case-2 waters. We suggest that it would be better to use the Case-2 algorithm if we want to get the quantitative analysis of chlorophyll *a* concentration. For qualitative analysis, the standard algorithm for Case-1 waters still can be used for the purpose to identify the high concentration area. The information is useful to understand the biological process occurring in the ocean. There is high concentration in the coastal area near the shoreline, but we cannot estimate exactly how much the concentration is.

3.2. Front, Upwelling and Eddies

The other information that can be extracted from chlorophyll *a* images is oceanographic processes such us fronts, eddies and upwelling. The satellite-derived SST images of thermal infrared bands are usually used for the observation of fronts a long time ago. However, in summer, increasing surface-heating effects make SST uniform and the SST front disappears.[13)]

We compared the chlorophyll *a* image (Plate 1a) and SST image (Plate 1b) deduced from the same MODIS data. From the chlorophyll *a* image, we could clearly see the front between coastal water and Kuroshio water, because the image showed different colors between them. In addition, when we made line transect (white line in Plate 1a) from the coastal area to the Kuroshio water area and extract the concentration value, the graph showed the high gradient of chlorophyll *a* concentration (Fig. 3). On the other hand, the SST image showed little difference among the surveyed areas, and it is difficult to see the front. Actually, we could not see the front from the SST gradient in the transect line (Fig. 3) and the temperature difference was only 2ºC. Comparing the locations of the Kuroshio front detected by satellite-derived chlorophyll *a* images with the in situ data, Takahashi and Kawamura[13)] concluded that the Kuroshio front detection method using chlorophyll *a* concentration works quite well in summer, when the SST images are less sensitive to detect the front.

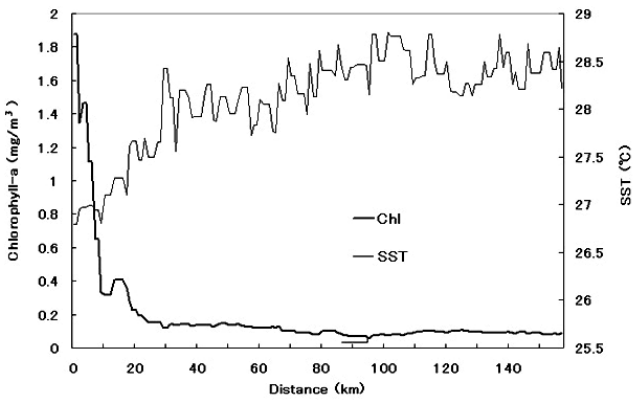

Fig. 3. Extracted value of chlorophyll *a* concentration and SST along the transect line in Plate 1a on the 27th July 2005.

Upwelling is a term describing the processes that causes the upward movement of seawater from the deeper layer into the surface layer. This process increases the primary production, since inorganic nutrients, which derive from decomposition of organic matters by heterotrophic organisms, are brought up from the deep ocean layer and accumulated in the surface layer. The nutrient supply stimulates primary productivity, which results in large fish production, and supports active fishing ground.[17] The upwelling process could be seen easily from chlorophyll *a* image that is shown in Plate 1c. In the east of Tanegashima Island, there are five circular spots with high chlorophyll *a* concentration. Several satellite data (AVHRR, CZCS, SeaWiFS, OCI) have been used to study the annual variations of DSU (Dongshan Upwelling) and TBU (Taiwan Bank Upwelling) zones in the Taiwan Strait during the summer season.[18] The present study demonstrates the potential of satellite data on upwelling monitoring for a long time period. The MODIS data, that is more sensitive than other ocean color data, show the upwelling phenomena clearly.

The generic term "eddies" used by physical oceanographers includes the meandering and filament of intense current systems, semi-attached and cast-off ring currents, advective vortices extending throughout the entire water column, lens vortices, planetary waves, topographic waves and wakes, etc. By temporal chlorophyll *a* images, we found eddies appearing in the study area as shown in Plate 2a. These eddies occurred almost in all seasons, especially in summer, these eddies appearred more frequently and were bigger than those in the other seasons. Ebuchi and Hanawa[19] suggested, based on SSH (Sea Surface Hight) variations, that eddy might be generated in Kuroshio extension region, and propagated westward to the Kuroshio re-circulation region. The intensive eddies during summer season might be due to the maximum volume transport of Kuroshio Current occurring in this season.[20] These eddies increase the chlorophyll *a* concentration, which is generated by water mixing of coastal waters with Kuroshio waters. The attractive increasing of chlorophyll *a* concentration can be seen in the comparison of concentrations between 27th July 2005 image (Plate 1a) and 14th September 2005 (Plate 2a) that is shown in Fig. 4. In Plate 2a, we can also see the chlorophyll *a* bloom from February to April.

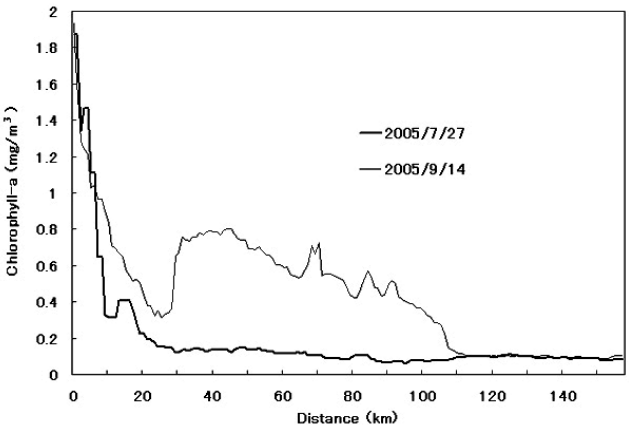

Fig. 4. Increase of the chlorophyll *a* concentration from the 27th July 2005 to 14th September 2005 due to eddies.

3.3. SST Distribution

Plate1b shows the SST distribution at the study area in summer. The SST was almost the same except the inside of Bungo Channel, where the effect of Kuroshio water is not so dominant, and the temperature in this area was about 23ºC. The SST in the coastal waters was about 27ºC just near the shoreline and then increased eastward to 28.5ºC in the Kuroshio water and then decreased again beyond Kuroshio water. This phenomenon indicates that the Kuroshio Current dominantly affects in the distribution of SST. In contrast, the SST distribution in winter is very different (Plate 1d). The Kuroshio Current can be seen, however the SST was as low as 18º - 21ºC. The low SST indicates that the Kuroshio Current is not dominant due to the minimum volume transport in this season.[20] The SST

distribution is affected by cooling due to the minimum heat flux during winter season with decreasing atmosphere temperature.

The dominant effect of the Kuroshio Current also can be seen in the correlation between chlorophyll *a* concentration and SST. Fig. 5a (summer) shows the high correlation in the Kuroshio region with $R^2 = 0.65$, indicating the Kuroshio Current effect was dominant. When the Kuroshio Current is dominant, the warm Kuroshio Current, which has high temperature but is low in chlorophyll *a* concentration, affects the SST distribution. If coastal water with low temperature and high chlorophyll *a* concentration mixes with Kuroshio water, the correlation will be high. On the other hand, in winter season (Fig. 5b), the correlation in the Kuroshio region was low with $R^2 = 0.17$. This means that the mixing between coastal water and Kuroshio water was weak and the distribution of SST was affected by atmospheric cooling due to the winter season. If there would be no mixing, decrease of water temperature would not increase the chlorophyll *a* concentration. In the coastal region, chlorophyll *a* concentration and SST showed high correlation both in summer ($R^2 = 0.55$) and in winter ($R^2 = 0.84$)

We have not emphasized SST as a control factor, although it certainly affects all-biological

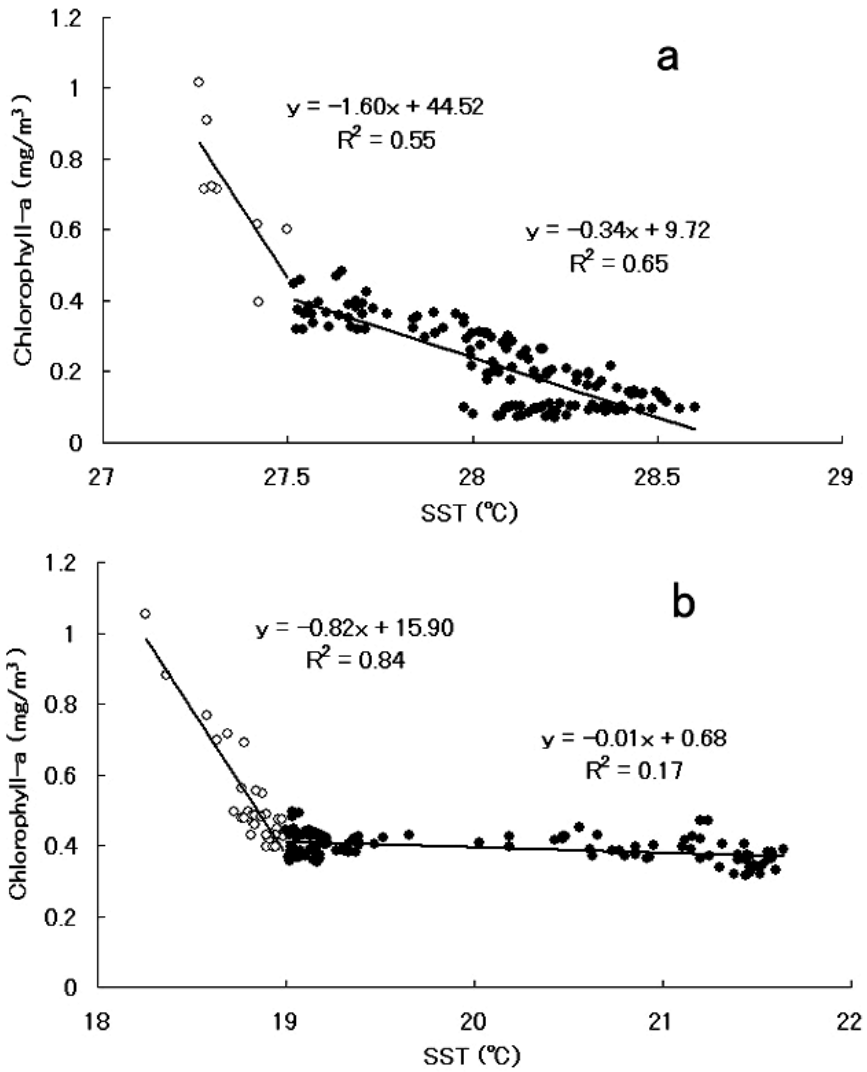

Fig. 5. Scatter diagram and correlation between the averaged chlorophyll *a* concentration and SST in summer (a) and in winter (b) in the transect line shown in Plate 1a. Open and closed circles indicate the data in the coastal and the Kuroshio-affected region, respectively.

transformations. The effects of light and nutrients are indeed important, but what we can see in primary production in the world waters differs much from what we might predict merely on the basis of variation of light and nutrients.[21)]

3.4. PIV

Recently, many studies on the observations of surface patterns from satellite images have been published. Leese *et al.*[12)] measured the cloud motion from satellite images and the motion of ice has been studied by Ninnis *et al.*[22)] and Ettema *et al.*[11)] In the ocean application, there were also many published papers, such as Emery *et al.*[23)], Kelly[24)], Gao and Lythe,[25)] and Wu *et al.*[26)] However, they used sea surface temperature deduced from infrared data. Vastano and Borders[27)] have examined sea surface motion over anti-cyclonic eddy, and Kamachi[28)] has developed a new approach of surface velocity measurement in the eddy rotation. In the preliminary study,[29)] we found that the chlorophyll *a* image deduced from MODIS data showed the surface feature in more detail than the SST image. The small and medium-scale eddies could be identified in the chlorophyll *a* image but could not be seen in the SST image. According to this result, we examined the possibility of velocity measurement using the chlorophyll *a* concentration image deduced from MODIS data.

After deciding the searching area as 61 x 61 pixels according to the mean value of the ocean current velocity from JODC and performing many experiments by using different sizes of interrogation, we got the pretty good result by 20 x 20 pixels of the interrogation area (Plate 2b(a)). However, this result showed only a few amount of vector lines and seems to present the movement of major water mass, not to show detailed movement in the whole area. Then we reduced the size of the interrogation area to 10 x 10 pixels and got Plate 2b(b), which seems to be a little complex and to include some errors. If we show only the vectors of the maximum correlation coefficient larger than 0.8 and omit the vectors going from the origin to the end of the interrogation area, we got the best result what we can do with many limitation of the data condition (Plate 2b(c)). The result was detailed and seems good for the visual interpretation of the water mass movement.

Comparing Plate 2b(a) with Plate 2b(c), we could see the difference of current directions caused by the difference of the interrogation area. The Plate 2b(a) showed the movement of large water volume movement that represents a major current occurring in this area i.e., Kuroshio Current. But we could not see the movement of the small water mass such as eddies and disturbances clearly. The figure Plate 2b(c) showed the movement of the smaller water mass, but still we could not see the details of the disturbance of water. Kamachi[28)] asserted that the cross correlation method could not detect rotation and deformation. Even if we use the better data to show the ocean feature, we still cannot see the more detailed result owing to the too long time interval. Emery *et al.*[23)] used very short time interval images (e.g., 4-5 hours) for the purpose to find rotational motion. Actually, the rotational motion could clearly be seen in the chlorophyll *a* images directly, but we could not derive the velocity of rotational motion. The resulting vector images of the PIV showed the indication of rotation by a disarrayed vector line structure.

3.5. Seasonal Change of Chlorophyll *a* Concentration

We examined the seasonal distribution characteristics of chlorophyll *a* concentration using the temporal data from April 2005 until March 2006. The spring season was represented by April–June 2005 data, the summer

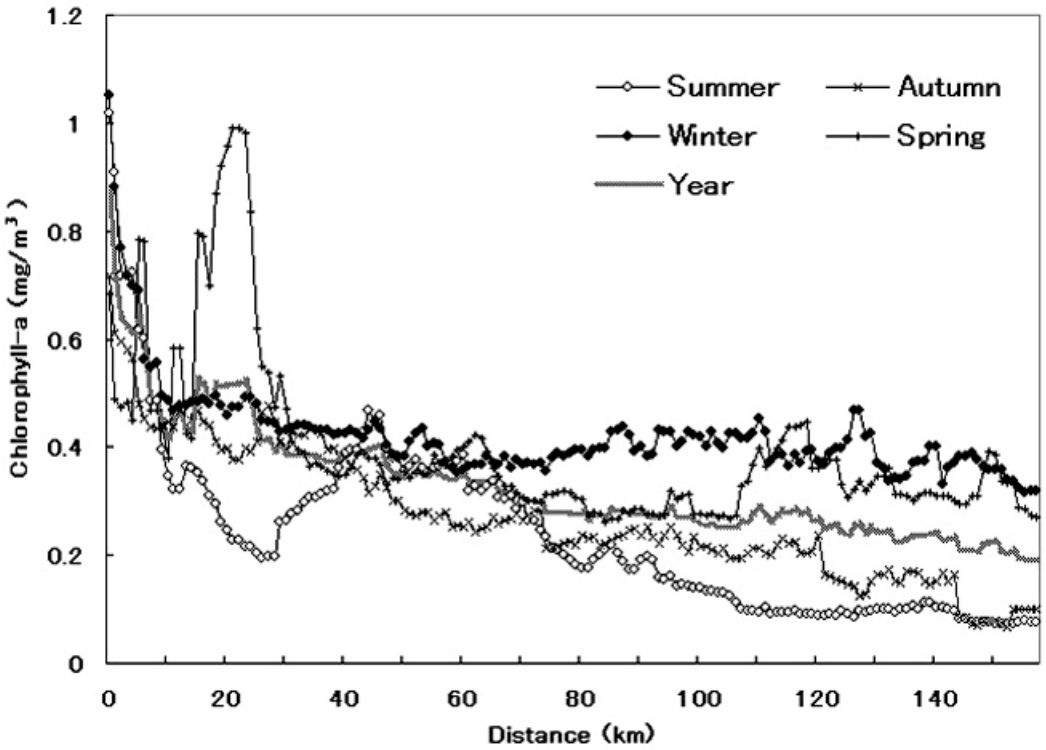

Fig. 6. Changes of the chlorophyll *a* concentrations along the transect line in Plate1a. The concentrations of spring, summer, autumn and winter seasons are averaged.

season was represented by July–September 2005, the autumn season was represented by October–December 2005 and the winter season was represented by January–March 2006. The averaged chlorophyll *a* concentration was calculated in each season and was shown in Fig. 6.

From the figure, we can divide the region into 4 sub-regions. The first is a coastal region just near the shoreline (up to about 10 km), where the chlorophyll *a* concentration is high and almost the same in all seasons. The dominant factor in this area is the nutrient supply from the land area. The second is a coastal region where the mixing by eddies was strong (from about 10 km to about 40 km). The coastal water was mixed with Kuroshio water due to eddies. The chlorophyll *a* concentration was very fluctuant depending on size and lifetime of the eddy. The third is a usually mixing area between coastal water and Kuroshio water (from about 40 km up to about 70 km). Although the difference was small, the chlorophyll *a* concentration was higher in winter and spring and lower in autumn. In summer 2005, a big eddy appeared and increased the chlorophyll *a* concentration up to almost the same quantity as in winter and spring. In this region the chlorophyll *a* concentration looks like to be the same in all season. The fourth is an ocean region (further than about 70 km) where the chlorophyll *a* concentration depends on the season and showed relatively high variation, higher in winter and spring, low in autumn and lower in summer.

4. Conclusion

These data will improve our understanding of global dynamics and processes occurring on the land, in the oceans, and in the lower atmosphere. MODIS is playing a vital role in the development of validated, global, interactive Earth system models, which are able to predict global change accurately enough to assist policy

makers in making sound decisions concerning the protection of our environment.

MODIS ocean color data is a useful tool to study oceanographic processes. The spatial distribution of chlorophyll *a* concentration could be calculated and the deduced concentration was nearly correct. Especially, the truly synoptic image of the chlorophyll *a* concentration and SST is really a great tool to understand the interaction process between temperature and biological process. In summer, we could see the front more clearly by chlorophyll *a* concentration images than by SST images. Eddies could be also interpreted well by chlorophyll *a* images. By PIV analysis using chlorophyll *a* images, the ocean flow field including direction and velocity of the current could be derived.

The chlorophyll *a* concentration was higher than 2 mg/m^3 inside Bungo channel, and higher than 0.5 mg/m^3 in just near the shoreline. Because of eddies, the coastal water and Kuroshio water were mixed and then the chlorophyll *a* concentration increased. In the Kuroshio axis the chlorophyll *a* concentration is low. Using temporal data, the seasonal changes of the chlorophyll *a* concentration were also examined. They were almost the same in the coastal area, and depended on eddies in the eddy region. In the mixing region, the chlorophyll *a* concentration was almost the same during the all seasons. In the region where Kuroshio water was dominant, the concentration were different in each season, higher in the winter and spring, low in autumn and lower in summer.

Acknowledgement

The authors are very grateful for freely using the data to Goddard Earth Science, Data and Information Service Center, the National Aeronautics and Space Administration (NASA), the United States of America. Also, we are very grateful for downloading and instruction of the SeaDAS software to Ocean Color Team and SeaDAS Support Service.

References

1) Mellor, G. L. (1996). Introduction to Physical Oceanography. Princeton University, Princeton, New Jersey: 3.
2) Cushman-Roisin, B. (1994). Introduction to geophysical fluid dynamics. Prentice Hall, Englewood Cliffs, New Jersey: 12-13:.
3) Campbell, J. B. (1996). Introduction to Remote Sensing, 2nd Ed. The Gulfford press, New York.
4) R. Vogel, (2002) http://modis-ocean.gsfc.nasa.gov/edu /researchintro/.
5) Zagaglia, C. R., J. A. Lorenzzetti and J. L. Stech (2004). Remote sensing data and long line catches of yellow fin tuna (*Thunus albacares*) in the equatorial Atlantic. *Remote Sens. Environ. J.,* **93**: 267-281.
6) Gomes, L. C., L. E. Miranda, and, A. A. Agostinho (2002). Fishery yield relative to chlorophyll *a* in reservoirs of the Upper Parana´ River, Brazil. *Fish. Res. J.,* **55**: 355-340.
7) Kawabe, M. (1995). Variation of current path, velocity, and volume transport of the Kuroshio in the relation with the large meander. *J. Phys. Oceanogr.,* **25**: 3103-3117.
8) Gordon, H. R., and M. Wang (1994). Retrieval of water-leaving radiance and aerosol optical thickness over the oceans with SeaWiFS: a preliminary algorithm. *Application. Opt.* **33**: 443-452.
9) Gordon, H. R. and K. J. Voss (1999). MODIS Normalized water-leaving radiance, Algorithm theoretical basis document. Departement of Physics Univesity of Miami.
10) Brown, O. B. (1994). MODIS Infrared Sea Surface Temperature Algorithm, Algorithm theoretical Basis Document Version 0, University of Miami.
11) Ettema, R., I. Fujita, M. Muste, and A. Kruger (1997). Particle image velocimetry for whole-field measurement of ice velocies. *Cold Regions Science and Technology,* **26**: 97-112.
12) Leese, J. A., C. S. Novak, and B. B. Clarke (1971). An automated technique for obtaining cloud motion from geo-synchronous satellite data using cross-correlation. *J. Appl. Meteorol.* **10**: 110-132.

13) Takahashi, W. and H. Kawamura (2005). Detection method of Kuroshio front using the satellite-derived chlorophyll a images. *Remote Sens. Environ. J.,* **97**: 83-91.

14) Miyasita, M. (2005). Bi-weekly to seasonal variability of satellite-derived chlorophyll a distribution: controlling factor in the ocean south of Honshu Island. *J. Remote Sens. Soc. Japan,* **25**(2): 169-178.

15) Carder, K. L., F. R. Chen, Zhongping Lee, S. K. Hawes, and J. P. Cannizzaro (2003). MODIS Ocean Science Team Algorithm Theoretical Basis Document. College of Marine Science University of South Florida

16) Darecki M., and D. Stramski (2004). An evaluation of MODIS and SeaWiFS bio-optical algorithms in the Baltic Sea. *Remote Sens. Environ.,* **89**: 326–350.

17) Takahashi, M. (2000). DOW: Deep Ocean water as our next natural resource. Terra Scientific Publishing Co., Tokyo 99.

18) Tang D. L., H. Kawamura , and L. Guan (2004). Long-time observation of annual variation of Taiwan Strait upwelling in summer season. *Adv. Space Res.,* **33**: 307-312

19) Ebuchi, N. and K. Hanawa (2000). Mesoscale eddies observed by TOLEX-ADCP and TOPEX/POSEIDON altimeter in the Kurosio recirculation region south of Japan. *J. Oceanogr.,* **56**: 43-57.

20) Ichikawa, H. and R. C. Beardsley (2002). The current system in the Yellow and East China Seas. *J. Oceanogr.,* **58**: 77-92.

21) Valialie, I. (1980). Ecology of Water Columns. In Fundamentals of Aquatic Ecology, edited by R.S.K. Barnes and K.M. Mann. Blackwell Scientific Publications: 29-56.

22) Ninnis, R. M. W. J. Emery, and M. J. Collins (1986). Automated extraction of pack ice motion from advanced very high-resolution radiometer imagery. *J. Geophys. Res.,* **91**: 10725-10.

23) Emery W. J., A. C. Thomas, M. J. Collins, W. R. Crawford, and D. L. Mackas (1986). An objective method for computing advective surface velocities from sequential infrared satellite images. *J. Geophys. Res.,* **91**(C11): 12865-12878.

24) Kelly, K. A. (1989). An inverse model for near-surface velocity from infrared images. *J. Phys. Oceanogr.,* **19**: 550-565.

25) Gao, J. and M. B. Lythe (1998). Effectiveness of the MCC method in detecting oceanic circulation patterns at a local scale from sequential AVHRR images. *Photogram. Engineer. Remote Sens.,* **64**(4): 301-308.

26) Wu, Q. X., D. Pariman, S. J. McNeil, and E. J. Barnes (1992). Computing advective velocities from satellite images of sea surface temperature. *IEEE Transact. Geosci. Remote Sens.,* **30**(1): 166-175.

27) Vastano, A. C., and S. E. Borders (1984). Sea surface motion over an anticyclonic eddy on the Oyashio Front. *Remote Sens. Environ.,* **16**: 87-90.

28) Kamachi, M. (1989). Advective surface velocities derived from sequential images for rotational flow field: Limitations and applications of Maximum Cross Correlation method with rotational registration, *J. Geophys. Res.,* **94**(C12): 18227-18233.

29) Winarso, G. and H. Kikukawa (2005). A Chlorophyll *a* distribution deduced by MODIS data and preliminary PIV application. Presented in Kagoshima University Remote Sensing Society Symposium (unpublished).

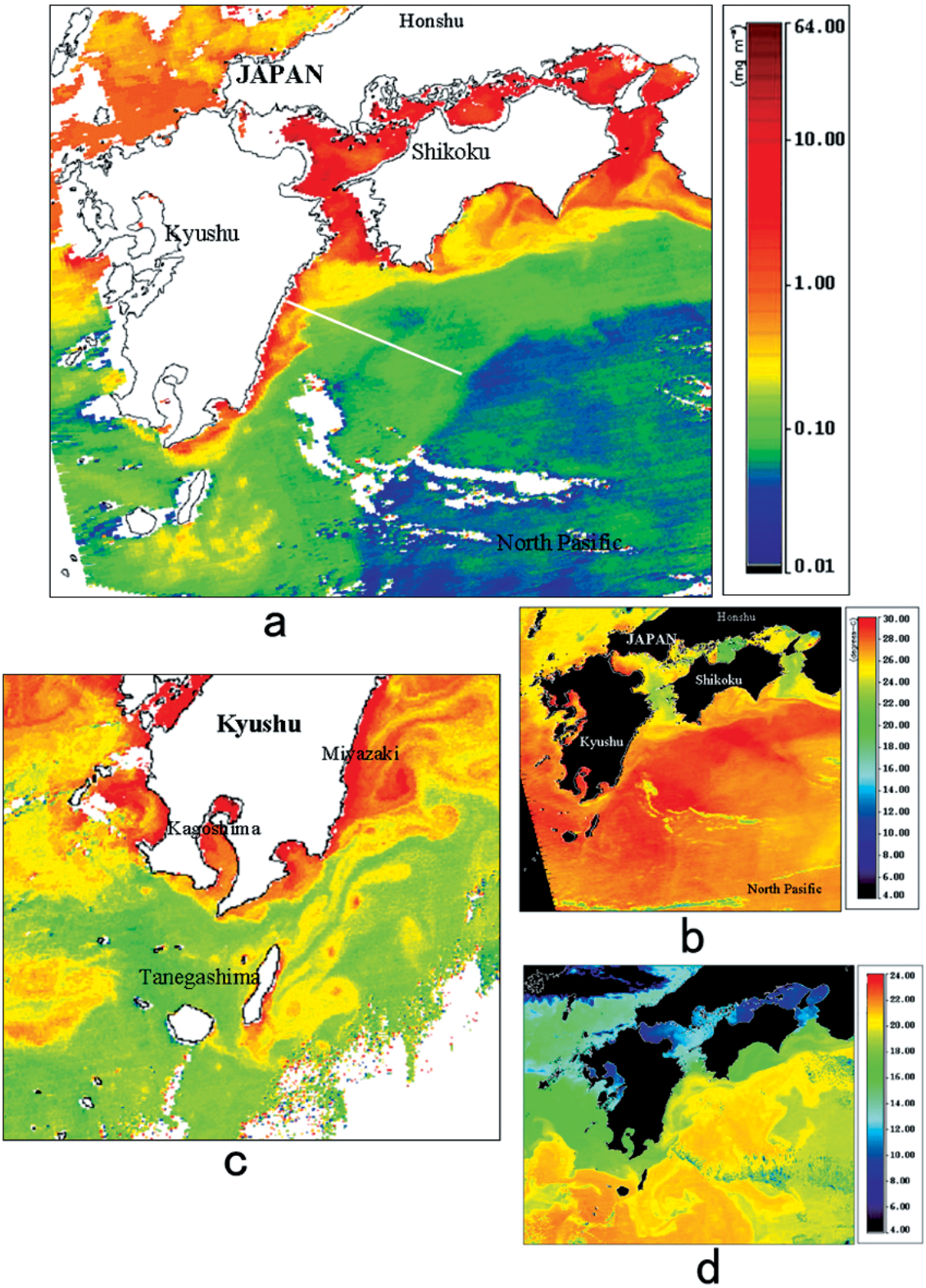

Plate. 1. **a:** MODIS-derived chlorophyll *a* concentration on 27th July 2005. White line denotes the transversal line used in Figs. 3 to 6. **b:** MODIS-derived SST on 27th July 2005. **c:** Chlorophyll *a* concentration on 18th October 2005. Five circular spots indicate the upwelling in the east of Tanegashima Island. The color scale is same as in Plate 1a. **d:** SST distribution image on 11th January 2005, the beginning of winter season.

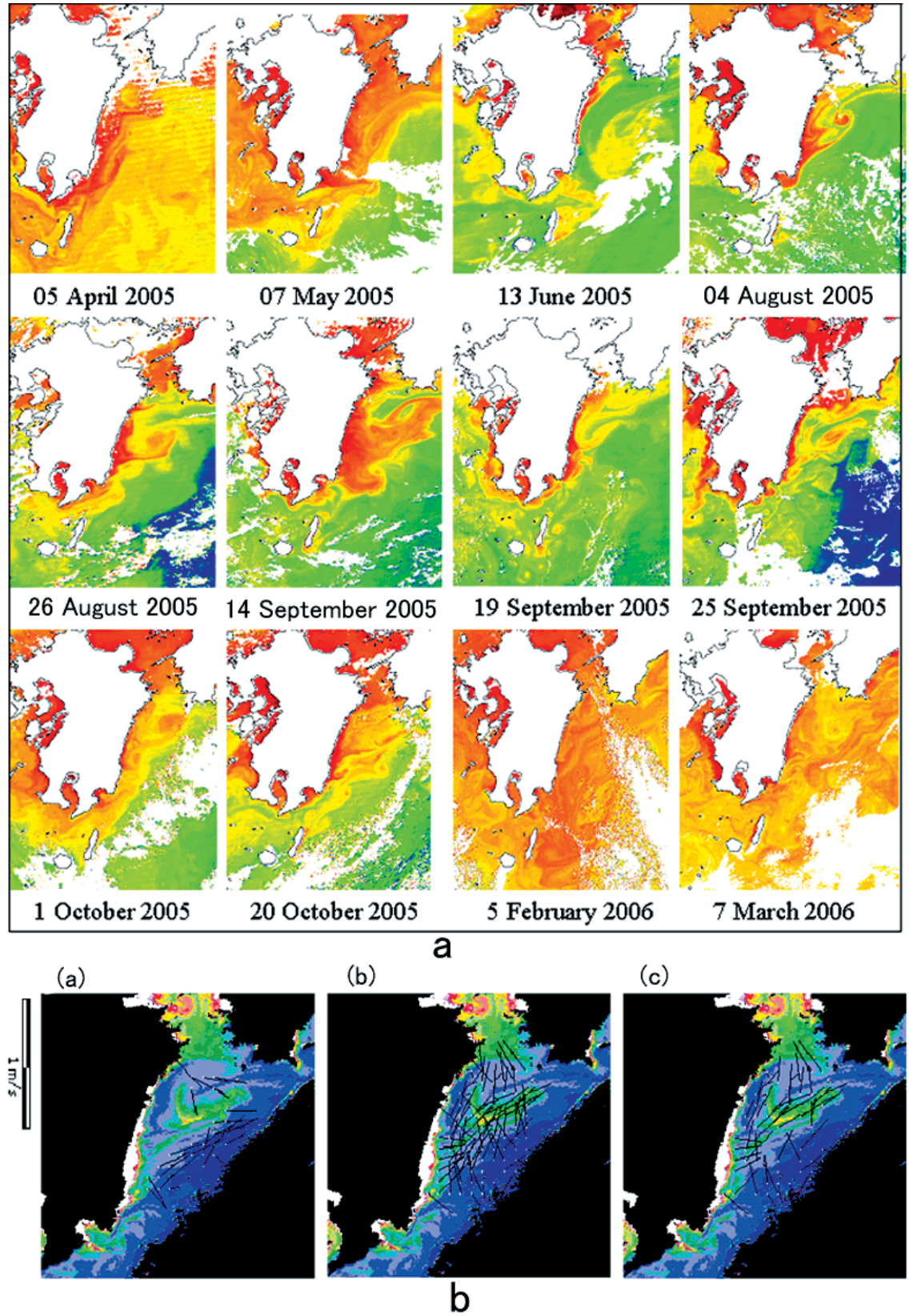

Plate. 2. **a:** Perennial chlorophyll *a* images, from April 2005 to March 2006. The color scale is the same as in Plate 1a. **b:** Results of PIV analysis. Small white points denote the beginning of the current vectors. (a) Major water mass movement. (b) Application of smaller interrogation area. Increase in the number of vectors is observed. (c) Application of an error correction. The maximum correlation coefficient is reduced.